URSI GASS 2021, Rome, Italy, 28 August - 4 September 2021

Empirical virtual height characteristics of ionospheric and ground scatter observed by the mid-latitude Christmas Valley SuperDARN HF radars

Evan G. Thomas* and Simon G. Shepherd
Thayer School of Engineering, Dartmouth College, Hanover, NH, USA

Abstract

The ground-based, high-frequency (HF) space weather radars of the Super Dual Auroral Radar Network (SuperDARN) utilize ionospheric refraction to routinely measure the Doppler velocity of backscatter echoes from *E*- and *F*-region plasma irregularities out to ranges of several thousand kilometers. An important byproduct of this sky-wave propagation is the occurrence of ground scatter echoes from land and ocean surfaces along the radar signal path. While these ground scatter returns are often treated as noise when producing global maps of ionospheric plasma motion, they can be useful for monitoring different geophysical phenomena such as traveling ionospheric disturbances or HF absorption caused by solar flares. In this study, we evaluate the accuracy of existing virtual height models used for geolocation of both ionospheric and ground backscatter using 5 years of data from the mid-latitude Christmas Valley SuperDARN radars, and propose new models suitable for correctly mapping both scatter types.

1 Introduction

Accurate geolocation of sky-wave radar signals requires reliable information of the ionospheric electron density distribution between the radar and backscattering volume [1]. Ray-tracing algorithms can be used to determine the propagation path of a high-frequency (HF) radar signal through the ionosphere by iteratively solving the Appleton-Hartree equation for the index of refraction [2]. Unfortunately, measurements of the ionospheric electron density profile are unavailable over much of the Earth, and climatological models such as the International Reference Ionosphere (IRI) [3] are unable to predict the highly variable conditions found within the auroral/polar ionosphere or at lower latitudes under disturbed geomagnetic conditions.

Two well-documented approaches have been developed for the geolocation of Super Dual Auroral Radar Network (SuperDARN) ionospheric scatter (IS) echoes. The first technique uses the measured range and the elevation angle calculated from the measured phase difference of the signal received at the primary and secondary antenna arrays to determine the virtual height of the scattering volume and therefore an estimate of the ground range [4, 5]. The second technique uses an empirical virtual height model (VHM) which varies as a function of range and assumes $\frac{1}{2}$-hop propagation [6]. Of the two approaches, the first technique using measured elevation information provides a more accurate ground range solution, however not all SuperDARN radars collect reliable elevation angle measurements due to issues such as hardware calibration [7, 8]. Therefore, the standard SuperDARN geolocation software uses an empirical VHM by default.

Neither of the above techniques as currently implemented in the SuperDARN geolocation software is appropriate for mapping ground scatter (GS) echoes to the Earth's surface. Furthermore, the existing SuperDARN VHMs were designed for mapping IS observed by the original high-latitude radars looking poleward into the auroral ionosphere and therefore may not be suitable for use with the more recently constructed mid-latitude radars [9]. Our goal is to develop an empirical VHM suitable for mapping mid-latitude SuperDARN IS and GS echoes to their correct ground range and geographic locations.

2 Data and Methodology

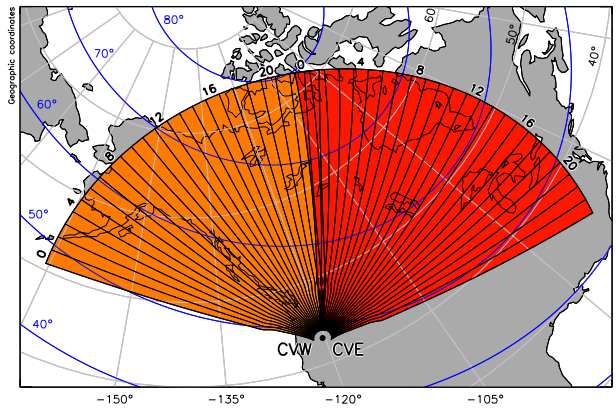

Figure 1. Nominal fields of view of the Christmas Valley West (CVW) and East (CVE) radars in geographic coordinates, shaded orange and red respectively. Selected azimuthal beam numbers are labeled for each radar and contours of constant geomagnetic latitude are overlaid in blue.

In this study we use 5 years (2014–2018) of data from the mid-latitude Christmas Valley East (CVE) and Christmas

Valley West (CVW) pair of co-located SuperDARN radars (Figure 1). More than 450 million backscatter measurements are available from each radar during this period, of which approximately 20% are identified as IS and 80% as GS echoes using the default SuperDARN criteria:

$$|v| + \frac{w}{3} < 30 \text{ m/s} \quad (1)$$

where v is the fitted Doppler velocity and w is the spectral width. Note that echoes from meteor trails at near-ranges or slow-moving IS may be mis-identified as GS using the simple empirical criteria of Equation 1.

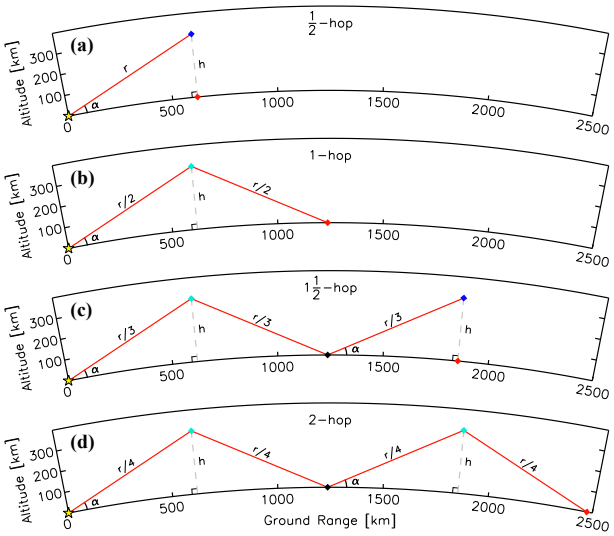

Figure 2. Schematic of (a) $\frac{1}{2}$-hop, (b) 1-hop, (c) $1\frac{1}{2}$-hop, and (d) 2-hop HF propagation geometries as a function of slant range r, elevation angle α, and virtual height h, assuming a spherical Earth with radius R_E. Blue diamonds indicate ionospheric backscatter locations, while red diamonds indicate the ground range associated with each ionospheric or ground backscatter location. Cyan and black diamonds indicate ionospheric and ground reflection points, respectively, while the yellow star at zero ground range indicates the radar location.

From the measured slant range r and elevation angle α, the corresponding virtual height h_N for any N-hop propagation mode (assuming a spherical Earth with radius R_E) can be found using:

$$h_N(r,\alpha) = \left[R_E^2 + \left(\frac{r}{2N}\right)^2 + \left(\frac{r}{N}\right) R_E \sin(\alpha)\right]^{1/2} - R_E \quad (2)$$

where integer values of N (e.g., 1, 2, 3, etc.) correspond to GS propagation modes while fractional values of N (e.g., $\frac{1}{2}$, $1\frac{1}{2}$, $2\frac{1}{2}$, etc.) correspond to IS propagation modes. The geometry of a few representative IS and GS propagation modes are shown in Figure 2 for an assumed F-region virtual height of 300 km. The ground range G_N to each IS or GS echo for any N-hop propagation mode can then be found using:

$$G_N(r,\alpha,h_N) = 2NR_E \sin^{-1}\left[\frac{\left(\frac{r}{2N}\right)\cos(\alpha)}{R_E + h_N}\right] \quad (3)$$

In this manner we can assess the accuracy of the standard SuperDARN VHM by comparing its ground range predictions for both IS and GS echoes to their true ranges obtained using Equations 2 and 3. It will therefore be important to identify the propagation mode of the HF backscatter echoes for correct ground range determinations. Note that for this summary paper, we will only show results from the CVE radar (although they are largely similar to the CVW results).

3 Results

The top row of Figure 3 shows the joint probability distribution of elevation angle and slant range mapped to virtual height observed by the CVE radar for IS (left column) and GS (right column) assuming a $\frac{1}{2}$-hop propagation mode, with the standard SuperDARN VHM overlaid in blue. Here the probability distributions have been normalized by the maximum occurrence in each range bin. For the IS shown in Figure 3a, the standard VHM correctly predicts the virtual height of the $\frac{1}{2}$-hop E-region scatter observed for slant ranges between 150 and 600 km. However, the virtual height of the F-region scatter observed beyond ~600 km slant range quickly rises away from the standard VHM prediction (which is fixed at 300 km) to greater virtual heights. Figure 3c shows the same distribution but assuming the IS observed beyond 2250 km is associated with a $1\frac{1}{2}$-hop F-region propagation mode, resulting in virtual heights closer to the standard VHM prediction at 300 km.

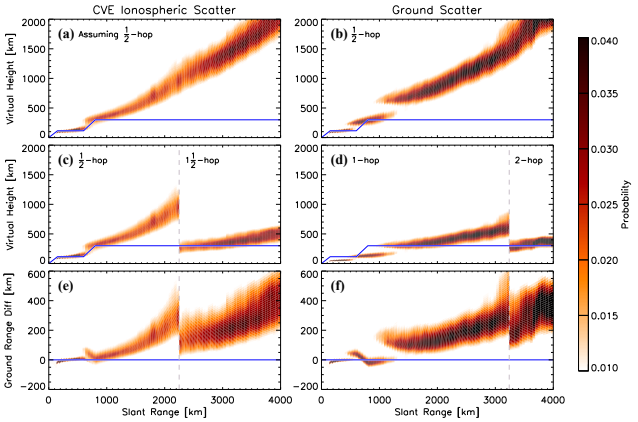

Figure 3. Normalized probability distribution of slant range and virtual height observed by the CVE radar for (a) ionospheric and (b) ground scatter assuming a $\frac{1}{2}$-hop propagation path, with the standard virtual height model overlaid in blue. (c) Same probability distribution for ionospheric scatter as panel (a) but assuming a $1\frac{1}{2}$-hop propagation mode for slant ranges beyond 2250 km (vertical dashed line). (d) Same probability distribution for ground scatter as panel (b) but assuming a 1-hop propagation mode for slant ranges up to 3240 km (vertical dashed line) and a 2-hop propagation mode for further ranges. Difference in ground ranges for (e) ionospheric and (f) ground scatter from panels (c) and (d) compared to application of the standard virtual height model; positive values indicate the true ground range is closer to the radar than suggested by the model.

For the GS shown in Figure 3b, a $\frac{1}{2}$-hop assumption should not yield an accurate virtual height unless the backscatter echoes have been mis-identified due to the criteria in Equation 1. The distribution observed between 100 and 500 km slant range is located at an unphysically low virtual height ($\sim$50 km) when mapped using a 1-hop assumption (Figure 3d), suggesting it is likely associated with backscatter from either meteor trails or E-region irregularities. Similarly, it is ambiguous whether the intermediate distribution located between 500 and 1200 km slant range belongs to either a $\frac{1}{2}$-hop F-region (IS) or 1-hop E-region (GS) propagation mode. Upon close examination of the statistical distributions, we have identified a likely transition from 1- to 2-hop F-region GS at $\sim$3240 km slant range.

The bottom row of Figure 3 shows the difference in ground range for the IS in Figure 3c and GS in Figure 3d when compared to using the standard VHM. In this way, we see how the standard VHM can incorrectly map $\frac{1}{2}$-hop F-region IS $\sim$50–400 km further from the radar than its actual distance, and $1\frac{1}{2}$-hop IS $\sim$100–600 km further away (Figure 3), depending on its slant range. Similarly, the standard VHM incorrectly places 1- and 2-hop GS $\sim$100–500 km further from the radar than its actual distance.

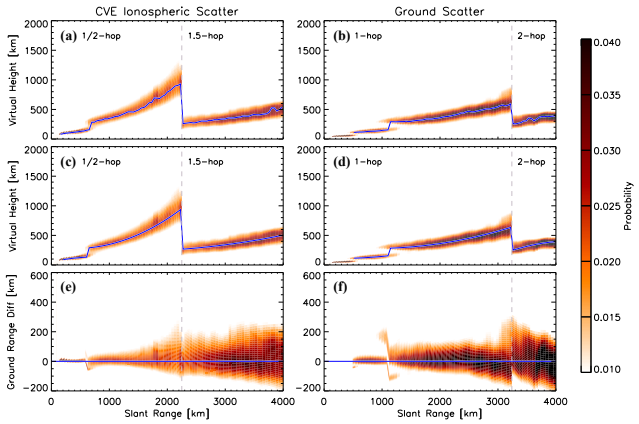

Figure 4. Normalized probability distribution of slant range and virtual height observed by the CVE radar for (a) ionospheric and (b) ground scatter using the same propagation assumptions as Figures 3c and 3d respectively, with the maximum occurrence at each range overlaid in blue. (c) Same probability distribution for ionospheric scatter as panel (a) but with the low-order polynomial fit to the maximum occurrence overlaid in blue. (d) Same probability distribution for ground scatter as panel (b) but with the low-order polynomial fit to the maximum occurrence overlaid in blue. Difference in ground ranges for (e) ionospheric and (f) ground scatter from panels (c) and (d) compared to application of the two new virtual height models; positive values indicate the true ground range is closer to the radar than suggested by the model.

To address these shortcomings of the standard VHM when applied to mid-latitude radar observations, we use these empirical results to derive two independent VHMs which can accurately geolocate IS and GS echoes, respectively. The top row of Figure 4 again shows the normalized probability distributions for IS and GS from Figures 3c and 3d, where the blue curve now indicates the maximum occurrence at each range bin. A new IS VHM is derived by fitting three low-order polynomials to the maximum occurrence of the $\frac{1}{2}$-hop E-region (160–650 km), $\frac{1}{2}$-hop F-region (650–2250 km), and $1\frac{1}{2}$-hop F-region ($>$ 2250 km) distributions (Figure 4c). Similarly, a new GS VHM is found by fitting three low-order polynomials to the maximum occurrence of the 1-hop E-region (520–1150 km), 1-hop F-region (1150–3240 km), and 2-hop F-region ($>$ 3240 km) distributions (Figure 4d). The bottom row of Figure 4 shows the resulting improvement in the ground ranges predicted by the new VHMs, where the distribution corresponding to each propagation mode is now centered about zero ground range error.

4 Summary

In this study, we have analyzed 5 years of data from the mid-latitude Christmas Valley East and West SuperDARN radars, consisting of more than 450 million backscatter echoes from each site. We have demonstrated how the virtual height and ground range for both ionospheric and ground scatter propagation modes can be calculated from the measured elevation angle and slant range for each backscatter echo. The standard SuperDARN virtual height model is shown to accurately determine the ground range of $\frac{1}{2}$-hop E-region echoes, however there is a systematic error in the ground range determination for $\frac{1}{2}$- and $1\frac{1}{2}$-hop ionospheric propagation modes placing the scattering volumes too far from the radar. Likewise, 1- and 2-hop F-region ground scatter propagation modes are also incorrectly mapped several hundred kilometers further away from the radar than their true location. We conclude by presenting two new virtual height models which are optimized for geolocating ionospheric and ground scatter propagation modes (specifically for mid-latitude radars).

5 Acknowledgements

This research was funded by the National Science Foundation (NSF) under grant OPP-1836426. The authors acknowledge the use of SuperDARN data. SuperDARN is a collection of radars funded by the national scientific funding agencies of Australia, Canada, China, France, Italy, Japan, Norway, South Africa, UK, and United States. The raw SuperDARN data are available from the British Antarctic Survey (BAS) SuperDARN data mirror (https://www.bas.ac.uk/project/superdarn).

References

[1] B. W. Reinisch, D. M. Haines, K. Bibl, I. Galkin, X. Huang, D. F. Kitrosser, G. S. Sales, and J. L. Scali, "Ionospheric sounding in support of over-the-horizon radar," *Radio Sci.*, **32**, 01, July 1997, pp. 1681–1694, doi:10.1029/97RS00841.

[2] R. M. Jones and J. J. Stephenson, "A versatile three-dimensional ray tracing computer program for radio waves in the ionosphere," *OTR 75–76*, October 1975.

[3] D. Bilitza, D. Altadill, Y. Zhang, C. Mertens, V. Truhlik, P. Richards, L.-A. McKinnell, and B. Reinisch, "The International Reference Ionosphere 2012 - a model of international collaboration," *J. Space Weather Clim.*, **4**, 20, February 2014, A07, doi:10.1051/swsc/2014004.

[4] S. G. Shepherd, "Elevation angle determination for SuperDARN HF radar layouts," *Radio Sci.*, **52**, 14, August 2017, pp. 938–950, doi:10.1002/2017RS006348.

[5] D. André, G. J. Sofko, K. Baker, and J. MacDougall, "SuperDARN interferometry: Meteor echoes and electron densities from groundscatter," *J. Geophys. Res.*, **103**, 01, April 1998, pp. 7003–7015, doi:10.1029/97JA02923.

[6] G. Chisham, T. K. Yeoman, and G. J. Sofko, "Mapping ionospheric backscatter measured by the SuperDARN HF radars – Part 1: A new empirical virtual height model," *Ann. Geophys.*, **26**, 13, May 2008, pp. 823–841, doi:10.5194/angeo-26-823-2008.

[7] R. A. Greenwald, N. Frissell, and S. de Larquier, "The importance of elevation angle measurements in HF radar investigations of the ionosphere," *Radio Sci.*, **52**, 03, March 2017, pp. 305–320, doi:10.1002/2016RS006186.

[8] G. Chisham, A. G. Burrell, A. Marchaudon, S. G. Shepherd, E. G. Thomas, and P. Ponomarenko, "Comparison of interferometer calibration techniques for improved SuperDARN elevation angles," *Polar Sci.*, 10, January 2021, doi:10.1016/j.polar.2021.100638.

[9] N. Nishitani, et al., "Review of the accomplishments of mid-latitude Super Dual Auroral Radar Network (SuperDARN) HF radars," *Prog Earth Planet Sci*, **6**, 18, March 2019, pp. 1–57, doi:10.1186/s40645-019-0270-5.